High emission power and Q factor in spin torque vortex oscillator consisting of FeB free layer

Sumito Tsunegi[1], Hitoshi Kubota[1], Kay Yakushiji[1], Makoto Konoto[1], Shingo Tamaru[1], Akio Fukushima[1], Hiroko Arai[1], Hiroshi Imamura[1], Eva Grimaldi[2], Romain Lebrun[2], Julie Grollier[2], Vincent Cros[2], and Shinji Yuasa[1]

[1]National Institute of Advanced Industrial Science and Technology (AIST), Spintronics Research Center, Tsukuba, Ibaraki 305-8568, Japan
[2]Unité Mixte de Physique CNRS/Thales and Université Paris Sud 11, 1 av. A. Fresnel, Palaiseau, France

Microwave oscillation properties of spin torque vortex oscillators (STVOs) consisting of an FeB vortex free layer were investigated. Because of a high MR ratio and large DC current, a high emission power up to 3.6 µW was attained in the STVO with a thin FeB free layer of 3 nm. In STOs with a thicker FeB layer, e.g., 10 nm thick, we obtained a large Q factor greater than 6400 while maintaining a large integrated emission power of 1.4 µW. Such excellent microwave performance is a breakthrough for the mutual phase locking of STVOs by electrical coupling.
© 2014 The Japan Society of Applied Physics

A spin torque oscillator (STO) is a device that transforms the magnetic precession motion excited by a spin transfer torque to the high-frequency electrical signal through the magneto-resistance (MR) effect.[1,2] Several types of STOs have been investigated to realize high emission power and high Q factor (narrow linewidth), both of which are necessary for practical applications such as nanoscale microwave generators and dynamic field sensors.[3] In STOs, the magnetization contained in a nanopillar structure,[1,2] a point contact structure,[4] or a confined structure[5] can be excited by the spin transfer effect, resulting in a uniform precession with a high frequency (~GHz). In the early stage of the study, the STOs made of metallic magnetoresistive elements were intended to perform only with a low emission power. To strongly enhance the emission power, we adopted MgO-based magnetic tunnel junctions (MTJs) in the STO, which was successful in combining both a higher power and a higher Q factor.[6–9] However the oscillation spectrum of this type of STO is greatly influenced by nonlinearity[10] (strong coupling between amplitude and phase in the magnetization precession) and thermal fluctuation, which eventually gives rise to the complexity (but also the richness) of oscillation dynamics.

Another type of STO, in which a magnetization vortex is formed in a free layer, has been investigated more recently.[11,12] In such a system, the spin transfer torque can excite the gyrotropic motion of the magnetization vortex core, which is converted to high-frequency electrical signals (typically several hundred MHz). This type of STO is called a spin torque vortex oscillator (STVO). In STVOs, because the coefficient of the nonlinearity is small, the linewidth becomes narrower compared with the case of uniform precession of magnetization.[13] As evidence of this, we observed a very narrow linewidth smaller than 300 kHz in the STVO using a thick Ni–Fe free layer (5–15 nm) with a relatively large diameter (~300 nm).[13,14] Because of its narrow linewidth, the STVO is an ideal device for the investigation of the bias dependence of the oscillation properties,[15,16] the temperature dependence of the linewidth,[17] and the amplitude of the nonlinearity.[13]

From the viewpoint of technological applications, the synchronization of STVOs with an injected RF current (injection locking) has been intensively studied with the objective of quantifying the experimental conditions and realizing the mutual phase locking[4,18] of STVOs.[14,19] Mutual phase locking is an important technology not only to enhance the emission power and improve the spectral coherence[20,21] but also for the realization of novel spintronics devices such as associative memories.[22,23] Because of a higher degree of freedom in device design, mutual phase locking by electric coupling is more applicable to the devices than that by magnetic coupling, in which the incorporable length is limited to the 100-nm scale.[18] In the existing injection locking experiments, STVOs exhibiting a small emission power (<5 nW) with Q factors of ~150 were typically used.[19] One of the main conclusions obtained was that enhancing both the emission power and the Q factors of each single STVO is beneficial in realizing the mutual phase locking by electrical coupling.

In this work, we developed STVOs consisting of an FeB free layer combined with a MgO tunnel barrier and a MgO capping layer. This combination was successful in achieving a larger emission power in the previous experiment involving the nanopillar STOs.[7] Here, we will also report how the main characteristics of the oscillation properties of the STVOs are changed when the free layer thickness is increased.

MTJ films with a stacking structure of buffer/PtMn(15)/$Co_{70}Fe_{30}$(2.5)/Ru(0.98)/CoFeB(3.0)/MgO(1.0)/FeB(d_{FeB})/MgO(1.1)/Ta/Ru (nm) were prepared by UHV magnetron sputtering. We know from previous studies that the MgO capping layer on the FeB layer leads to a substantial decrease of the damping constant ($\alpha = 0.005$ for 2-nm-thick FeB),[24,25] which causes a reduction in the threshold current of the microwave emission.[15] In this study, the FeB thicknesses d_{FeB} were varied from 2.0 to 10.0 nm. After annealing at 360 °C in a vacuum, we measured the resistance–area products (RA) of the MTJs using the current-in-plane tunneling technique. The RA value slightly decreased from 3.7 to 3.1 Ω µm² with increasing d_{FeB}. The films were patterned into MTJs, each with a diameter of 300 nm, in order to stabilize the magnetization vortex in the FeB film. High-frequency signals were measured at room temperature using a real-time oscilloscope (20 GS/s, sampling time = 200 µs) with a DC bias voltage (V_{dc}) between 0 and +450 mV. The positive voltage sign corresponds to electrons flowing from the top FeB free layer to the bottom CoFeB reference layer. The observed time domain signals were transformed to the power spectral density (PSD).

Figures 1(a)–1(d) show the MR curves measured by sweeping the in-plane magnetic field applied parallel to the easy axis of the reference layer for the four different MTJs. The MR ratios were found to be approximately 125% in all
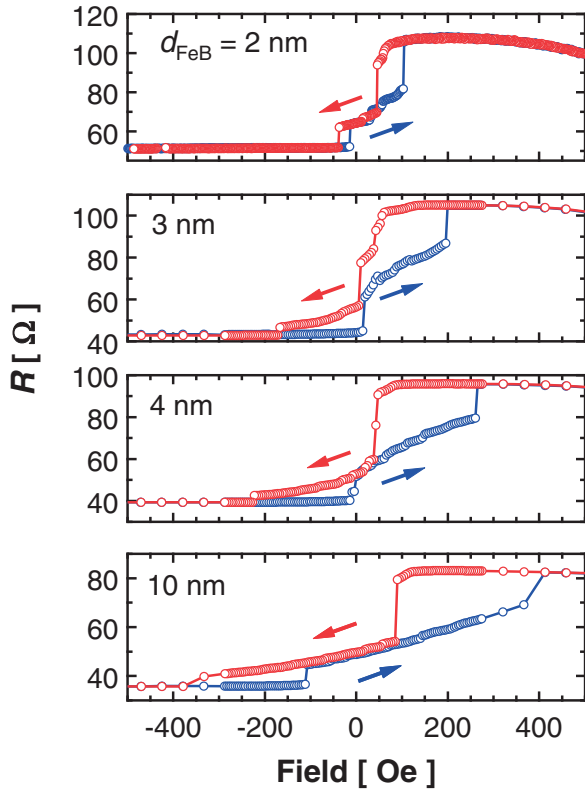
Fig. 1. Magnetoresistance curves of the STVOs with $d_{FeB} = 2$–10 nm measured under in-plane magnetic fields. The blue (red) shows the result observed by sweeping the magnetic field up (down).

Fig. 2. The out-of-plane magnetic field dependence of (a) emission power, (b) frequency (f_{osc}), and (c) linewidth (Δf) of the STVO with $d_{FeB} = 3$ nm at $V_{dc} = 450$ mV. The spectrum exhibiting (d) maximum emission power and (e) minimum linewidth obtained at the fields are indicated by open and closed arrows in (a) and (c), respectively.

ranges of thickness d_{FeB}. The steep change of resistance at a lower (higher) field corresponds to the magnetic field at which the magnetization vortex is created (annihilated). Linear resistance changes observed between the steep resistance changes at low and high fields are a typical magnetization process in which a magnetic vortex configuration is first nucleated.[26] The annihilation field increased as d_{FeB} was increased, which clearly shows that the magnetic vortex is more stable in the thicker FeB free layers.

When the reference layer had a uniform magnetization, a vortex core oscillation with a large amplitude was generated for the case where the z component (film normal) of the spin polarization of the current (p_z) parallel to the core polarity becomes sufficiently large.[27] In our experiment, p_z can be increased by increasing the tilt of the reference layer magnetization, which is induced by applying out-of-plane magnetic fields (H_{op}). Therefore, we measured the oscillation properties by changing H_{op} from +6 to −6 kOe. Figures 2(a) and 2(b) show the magnetic field dependence of the emission power (integrated power) and the oscillation frequency of the STVO with $d_{FeB} = 3$ nm at a high bias voltage ($V_{dc} = 450$ mV), respectively. The emission power was almost zero near zero field. With increasing (decreasing) H_{op}, the emission power abruptly increased and exhibited a maximum (P_{max}) at +1.9 kOe (−1.4 kOe). Hereafter, we designate the field where the emission exhibits a maximum as H_{Pmax}. Further increasing (decreasing) H_{op}, the emission power decreased gradually and reached zero at $|H_{op}| = 5.5$ kOe, which was identical to the saturation field (H_{sat}^{free}) of the FeB free layer. The field dependence of the emission power agreed well with previous reports[27] indicating that the vortex oscillation was excited

in the FeB free layer. Figure 2(d) shows the PSD spectrum corresponding to P_{max}, which is indicated by the open arrow in the figure. The spectrum exhibits a large and narrow peak, representing a Q factor of 171. The emission power reached 3.6 μW, which is the largest value yet reported among all types of STO.

The field dependence of the oscillation frequency (f_{osc}) is shown in Fig. 2(b). f_{osc} was increased gradually from approximately 200 to 400 MHz by increasing the magnitude of H_{op}. When $|H_{OP}|$ became larger than $H_{sat}^{free} = 5.5$ kOe, f_{osc} increased rapidly. Such field dependence was reported in the previous investigation.[27] We observed almost the same field dependence of the oscillation properties in other d_{FeB}.

Table I summarizes the observed values of P_{max} with corresponding experimental parameters for various FeB thicknesses. The values of the Ni–Fe STVO are also shown.[13] When $d_{FeB} \geqq 3$ nm, the integrated power decreased, while H_{Pmax} increased with increasing d_{FeB}. These results were explained by considering the increase in the damping torque, which is proportional to the magnetic moment: larger p_z with larger H_{op} is necessary to excite the vortex oscillation in thicker FeB. Note that the emission power for $d_{FeB} = 2$ nm was smaller than that for $d_{FeB} = 3$ nm. At $d_{FeB} = 2$ nm, we observed the quasi-uniform oscillation when applying strong magnetic fields of $|H_{OP}| \geq 3$ kOe. Under these conditions, f_{osc} increased with the field strength, similarly to Kittel's mode (not shown). These results indicate that the vortex core in the free layer for $d_{FeB} = 2$ nm was unstable compared with that for $d_{FeB} = 3$ nm. The instability of the vortex-core is the reason for the small emission power for $d_{FeB} = 2$ nm.

A semi-quantitative analysis based on the nonlinear auto-oscillator model given in Ref. 13 shows that the origin of

Table I. Experimental parameters of the STVOs with FeB free layers of $d_{FeB} = 2–10$ nm. Resistance (R), magnetoresistance ratio (MR), and current (I) represent the values measured at $V_{dc} = 450$ mV by applying the magnetic field of H_{Pmax}. Ni–Fe represents the STVO with Ni–Fe free layer.[13] The figures in parentheses show ratios of the parameter values of the FeB free layer to those of Ni–Fe free layer.

		R (Ω)	$\dfrac{50R_{Parallel}^2}{2(50+R)^2}$	MR (%)	I (mA)	H_{Pmax} (kOe)	H_{sat}^{ref} (kOe)	H_{sat}^{free} (kOe)	P' (μW)	P_{max} (μW)	S_0
(A)	FeB 2 nm	60	5.6 (0.9)	61 (3.6)	7.4 (2.0)	0.3	15	1.6	12 (52)	0.6 (26)	0.23
(B)	FeB 3 nm	55	4.3 (0.7)	77 (4.5)	8.2 (2.2)	1.9	15	5.8	17 (74)	3.6 (146)	0.46
(C)	FeB 4 nm	51	3.9 (0.6)	77 (4.5)	8.8 (2.3)	2.3	15	9.0	19 (81)	3.2 (128)	0.42
(D)	FeB 10 nm	47	3.6 (0.6)	63 (3.7)	9.5 (2.5)	1.8	15	14.4	14 (62)	1.7 (67)	0.34
(E)	Ni–Fe 5 nm[13]	55	6.2	17	3.8	4.5	15	8.1	0.2	0.025	0.33

the large emission power in our STVOs can be attributed to the large MR ratio and the ability to carry large current. According to Ref. 13, the emission power (P) is expressed as

$$P = \frac{50R_{parallel}^2}{2(50+R)^2}$$
$$\times \frac{I^2 MR^2}{4}\beta^2 \left[1 - \left(\frac{H_{op}}{H_{sat}^{ref}}\right)^2\right]\left[1 - \left(\frac{H_{op}}{H_{sat}^{free}}\right)^2\right]s_0^2$$
$$= P's_0^2, \tag{1}$$

where R, MR, and I represent the resistance, magnetoresistance ratio, and current, respectively. $R_{parallel}$ is the resistance at the parallel magnetic configuration. β is the conversion factor for converting the vortex core displacement into the change in the magnetization configuration, which is fixed to 2/3.[13,28] H_{sat}^{ref} is a magnetic field required to saturate the magnetization of the reference layer perpendicular to the film plane. The parameter s_0 is a ratio of the radius of the nanopillars and the radius of the vortex-core circular motion, the latter of which is determined by the competition between the spin transfer torque and damping torque. The experimental values of these parameters of the FeB STVOs and Ni–Fe STVO are presented in Table I.[13] We compare the parameters between the STVO with $d_{FeB} = 3$ nm (B) and those of the Ni–Fe STVO with $d_{NiFe} = 10$ nm (E). The observed emission powers were 3.6 μW and 25 nW for (B) and (E), respectively, corresponding to a ratio of 146. The MR ratio of device (B) (77%) was approximately 4.5 times larger than that of (E) (17%). In addition, the injected current of (B) (8.2 mA) was approximately 2.2 times larger than that of (E) (3.8 mA). These enhancements greatly contributed to the large ratio P' of 74 between (B) and (E). Similarly, in (A), (C), and (D), the P' ratios were very large (52–81). Because all of the parameters except for MR and I were similar in (A)–(E), the enhancement of P' in the FeB STVOs originated mainly from their large MR ratio and ability to carry large current. We should notice that the ratios of P' calculated for (B) and (C) were smaller than those of the observed P_{max}. The differences can be attributed to the change in the normalized oscillation radius s_0. The values of s_0 estimated by comparing the observed P_{max} with the calculated P' were 0.23, 0.46, 0.42, 0.34, 0.33 for devices (A)–(E), respectively, as shown in Table I. s_0 was the largest in (B) among all samples, indicating that effective excitation of the vortex
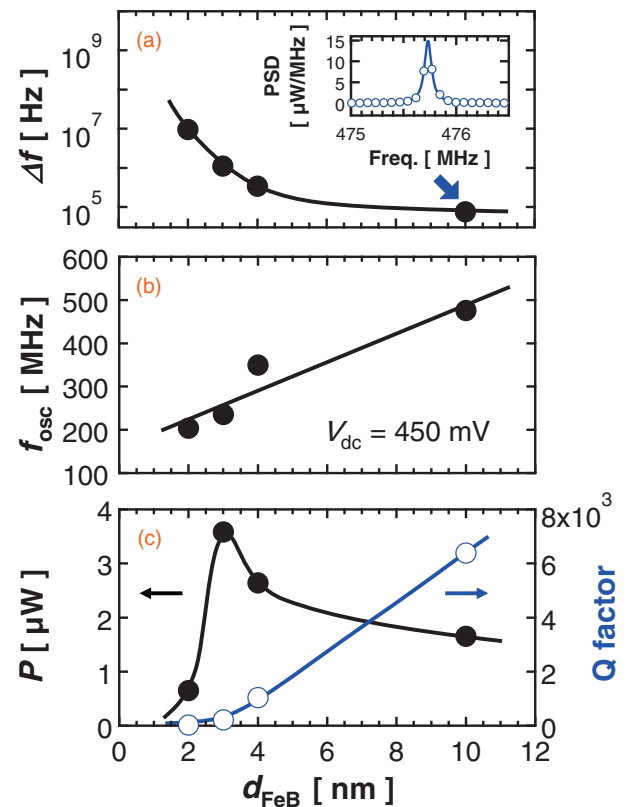
Fig. 3. The FeB thickness dependence of (a) linewidth, (b) oscillation frequency, and (c) emission power and Q factor obtained at H_{op}, where the linewidth was minimum. Inset in (a) shows the magnified PSD spectrum with a Lorentz function fit of the STVO with $d_{FeB} = 10$ nm.

motion was achieved in the thin free layer. s_0 decreased with increasing d_{FeB}, which is consistent with the expectation that the spin transfer torque that drives the vortex motion becomes less efficient in the thicker free layer.

Figure 2(c) shows Δf as a function of H_{op}. Δf exhibits minima of 1.1 MHz and 874 kHz at $H_{op} = 2.1$ and -1.1 kOe, respectively. The spectrum at $H_{op} = 2.1$ kOe is shown in Fig. 2(e) for example, representing a Q factor of 212. We obtained similar H_{OP} dependences of Δf in the STVOs with other FeB thicknesses. In Figs. 3(a)–3(c), we show the FeB thickness dependence of the linewidth Δf, oscillation frequency f_{osc}, integrated emission power P, and Q factor at H_{OP}, where the linewidth exhibits a minimum value. The Δf (f_{osc}) decreased (increased) with increasing d_{FeB} owing to the

enhancement of the vortex energy.[15] The emission power, which was largest (3.4 μW) at $d_{FeB} = 3$ nm, decreased with increasing d_{FeB}. In the case of $d_{FeB} = 10$ nm, Δf decreased to 74 kHz, and the Q factor remarkably increased to 6400 ($f_{osc} = 475$ MHz) at $H_{op} = 2.43$ kOe and $V_{dc} = 450$ mV, as shown in the inset of Fig. 3(a). The observed emission power and Q factor are much higher than any yet reported.

Let us briefly discuss the application of the FeB STVOs exhibiting high emission power and high Q factor for mutual synchronization. For the observation of the injection locking, an RF current typically on the order of 100 μA was injected into an STO with an impedance of typically 50 Ω, corresponding to an RF power of 0.5 μW. To realize mutual phase locking, the emission power of a single STVO should be larger than 0.5 μW. The observed emission power, shown in Fig. 3(c) ($d_{FeB} = 3$ nm), is at least three times larger than the required value. Concerning the Q factor, it is presently difficult to estimate the required value for mutual phase locking. Although STOs with a low Q factor (∼20) were injection-locked to an RF input current,[29] the STO with a higher Q factor exhibited a larger locking range.[20] Therefore, we expect that a robust mutual phase locking will be realized by STVOs with a high Q factor. The observed Q factor of 6400, which is far higher than that in previous reports, is greatly advantageous for mutual phase locking.

In summary, we investigated the oscillation properties of STVOs using an FeB vortex with various thicknesses. A very high emission power of 3.4–3.6 μW and a high Q factor of 212–171, correspondingly, were observed for $d_{FeB} = 3$ nm. The emission power decreased, while the Q factor increased with increasing d_{FeB}. In the case of $d_{FeB} = 10$ nm, we observed a Q factor of 6400 maintaining a high emission power of 1.4 μW. Using the high-performance STVOs, we anticipate the demonstration of mutual synchronization between multiple STOs, which may lead to a breakthrough in the development of new types of STO-based devices.

1) S. I. Kiselev, J. C. Sankey, I. N. Krivorotov, N. C. Emley, R. J. Schoelkopf, R. A. Buhrman, and D. C. Ralph, Nature **425**, 380 (2003).
2) W. H. Rippard, M. R. Pufall, S. Kaka, T. J. Silva, and S. E. Russek, Phys. Rev. B **70**, 100406(R) (2004).
3) K. Kudo, T. Nagasawa, K. Mizushima, H. Suto, and R. Sato, Appl. Phys. Express **3**, 043002 (2010).
4) S. Kaka, M. R. Pufall, W. H. Rippard, T. J. Silva, S. E. Russek, and J. A. Katine, Nature **437**, 389 (2005).
5) H. Suzuki, H. Endo, T. Nakamura, T. Tanaka, M. Doi, S. Hashimoto, H. N. Fuke, M. Takagishi, H. Iwasaki, and M. Sahashi, J. Appl. Phys. **105**, 07D124 (2009).
6) A. M. Deac, A. Fukushima, H. Kubota, H. Maehara, Y. Suzuki, S. Yuasa, Y. Nagamine, K. Tsunekawa, D. D. Djayaprawira, and N. Watanabe, Nat. Phys. **4**, 803 (2008).
7) H. Kubota, K. Yakushiji, A. Fukushima, S. Tamaru, M. Konoto, T. Nozaki, S. Ishibashi, T. Saruya, S. Yuasa, T. Taniguchi, H. Arai, and H. Imamura, Appl. Phys. Express **6**, 103003 (2013).
8) H. Maehara, H. Kubota, Y. Suzuki, T. Seki, K. Nishimura, Y. Nagamine, K. Tsunekawa, A. Fukushima, A. M. Deac, K. Ando, and S. Yuasa, Appl. Phys. Express **6**, 113005 (2013).
9) H. Maehara, H. Kubota, Y. Suzuki, T. Seki, K. Nishimura, Y. Nagamine, K. Tsunekawa, A. Fukushima, H. Arai, T. Taniguchi, H. Imamura, K. Ando, and S. Yuasa, Appl. Phys. Express **7**, 023003 (2014).
10) V. Tiberkevich, A. Slavin, and J. V. Kim, Appl. Phys. Lett. **91**, 192506 (2007).
11) V. S. Pribiag, I. N. Krivorotov, G. D. Fuchs, P. M. Braganca, O. Ozatay, J. C. Sankey, D. C. Ralph, and R. A. Buhrman, Nat. Phys. **3**, 498 (2007).
12) K. Miyake, Y. Okutomi, H. Tsukahara, H. Imamura, and M. Sahashi, Appl. Phys. Express **6**, 113001 (2013).
13) E. Grimaldi, A. Dussaux, P. Bortolotti, J. Grollier, G. Pillet, A. Fukushima, H. Kubota, K. Yakushiji, S. Yuasa, and V. Cros, Phys. Rev. B **89**, 104404 (2014).
14) A. Hamadeh, N. Locatelli, V. V. Naletov, R. Lebrun, G. de Loubens, J. Grollier, O. Klein, and V. Cros, Appl. Phys. Lett. **104**, 022408 (2014).
15) A. V. Khvalkovskiy, J. Grollier, A. Dussaux, K. A. Zvezdin, and V. Cros, Phys. Rev. B **80**, 140401(R) (2009).
16) A. Dussaux, A. V. Khvalkovskiy, P. Bortolotti, J. Grollier, V. Cros, and A. Fert, Phys. Rev. B **86**, 014402 (2012).
17) P. Bortolotti, A. Dussaux, J. Grollier, V. Cros, A. Fukushima, H. Kubota, K. Yakushiji, S. Yuasa, K. Ando, and A. Fert, Appl. Phys. Lett. **100**, 042408 (2012).
18) F. B. Mancoff, N. D. Rizzo, B. N. Engel, and S. Tehrani, Nature **437**, 393 (2005).
19) A. Dussaux, A. V. Khvalkovskiy, J. Grollier, V. Cros, A. Fukushima, M. Konoto, H. Kubota, K. Yakushiji, S. Yuasa, K. Ando, and A. Fert, Appl. Phys. Lett. **98**, 132506 (2011).
20) B. Georges, J. Grollier, V. Cros, and A. Fert, Appl. Phys. Lett. **92**, 232504 (2008).
21) J. Grollier, V. Cros, and A. Fert, Phys. Rev. B **73**, 060409(R) (2006).
22) G. Csaba, M. Pufall, D. E. Nikonov, G. I. Bourianoff, A. Horvath, T. Roska, and W. Porod, 13th Int. Workshop Cellular Nanoscale Networks and Their Applications (CNNA), 2012, p. 1.
23) N. Locatelli, V. Cros, and J. Grollier, Nat. Mater. **13**, 11 (2014).
24) M. Konoto, H. Imamura, T. Taniguchi, K. Yakushiji, H. Kubota, A. Fukushima, K. Ando, and S. Yuasa, Appl. Phys. Express **6**, 073002 (2013).
25) S. Tsunegi, H. Kubota, S. Tamaru, K. Yakushiji, M. Konoto, A. Fukushima, T. Taniguchi, H. Arai, H. Imamura, and S. Yuasa, Appl. Phys. Express **7**, 033004 (2014).
26) T. S. Machado, M. Argollo de Menezes, T. G. Rappoport, and L. C. Sampaio, J. Appl. Phys. **109**, 093904 (2011).
27) A. Dussaux, B. Georges, J. Grollier, V. Cros, A. V. Khvalkovskiy, A. Fukushima, M. Konoto, H. Kubota, K. Yakushiji, S. Yuasa, K. A. Zvezdin, K. Ando, and A. Fert, Nat. Commun. **1**, 8 (2010).
28) K. Y. Guslienko, B. A. Ivanov, V. Novosad, Y. Otani, H. Shima, and K. Fukamichi, J. Appl. Phys. **91**, 8037 (2002).
29) M. Quinsat, J. F. Sierra, I. Firastrau, V. Tiberkevich, A. Slavin, D. Gusakova, L. D. Buda-Prejbeanu, M. Zarudniev, J.-P. Michel, U. Ebels, B. Dieny, M.-C. Cyrille, J. A. Katine, D. Mauri, and A. Zeltser, Appl. Phys. Lett. **98**, 182503 (2011).